Anal Bioanal Chem (2013) 405:2535–2544
DOI 10.1007/s00216-012-6677-0

ORIGINAL PAPER

An evaluation of the capability of a biolayer interferometry biosensor to detect low-molecular-weight food contaminants

Terry F. McGrath · Katrina Campbell · Terry L. Fodey · Richard O'Kennedy · Christopher T. Elliott

Received: 22 October 2012 / Revised: 14 December 2012 / Accepted: 18 December 2012 / Published online: 22 January 2013

Abstract The safety of our food is an essential requirement of society. One well-recognised threat is that of chemical contamination of our food, where low-molecular-weight compounds such as biotoxins, drug residues and pesticides are present. Low-cost, rapid screening procedures are sought to discriminate the suspect samples from the population, thus selecting only these to be forwarded for confirmatory analysis. Many biosensor assays have been developed as screening tools in food contaminant analysis, but these tend to be electrochemical, fluorescence or surface plasmon resonance based. An alternative approach is the use of biolayer interferometry, which has become established in drug discovery and life science studies but is only now emerging as a potential tool in the analysis of food contaminants. A biolayer interferometry biosensor was assessed using domoic acid as a model compound. Instrument repeatability was tested by simultaneously producing six calibration curves showing replicate repeatability (n=2) ranging from 0.1 to 6.5 % CV with individual concentration measurements (n=12) ranging from 4.3 to 9.3 % CV, giving a calibration curve midpoint of 7.5 ng/ml (2.3 % CV (n=6)). Reproducibility was assessed by producing three calibration curves on different days, giving a midpoint of 7.5 ng/ml (3.4 %CV (n=3)). It was further shown, using assay development techniques, that the calibration curve midpoint could be adjusted from 10.4 to 1.9 ng/ml by varying assay parameters before the simultaneous construction of three calibration curves in matrix and buffer. Sensitivity of the assay compared favourably with previously published biosensor data for domoic acid.

Keywords Biolayer interferometry (BLI) · Label-free optical biosensor · Low-molecular-weight food contaminants · Concentration analysis · Shellfish analysis · Domoic acid

T. F. McGrath (✉) · K. Campbell · C. T. Elliott
ASSET Technology Centre, Institute for Global Food Security, School of Biological Sciences, Queen's University Belfast, Stranmillis Road,
Belfast BT9 5AG, Northern Ireland
e-mail: terry.mcgrath@qub.ac.uk

T. L. Fodey
Agri-food and Biosciences Institute, Stoney Road,
Belfast BT4 3SD, Northern Ireland

R. O'Kennedy
School of Biotechnology, Dublin City University,
Dublin 9, Ireland

Introduction

The safety of our food supply is of paramount importance in the fight to protect humans from exposure to infectious agents such as *Escherichia coli* [1] and banned veterinary drugs such as chloramphenicol which can cause conditions such as aplastic anaemia [2, 3]. Low-level exposure of pharmaceuticals can also threaten the continued viability of the therapeutic response through drug sensitisation [4] and antimicrobial resistance [5]. Thus, a wide range of monitoring tools have been developed and employed to detect trace levels of contaminants. One such technique is the use of biosensors to screen for food contaminants. A biosensor can be defined as a self-contained integrated device consisting of a biological binding partner, e.g. antibody, maintained in close spatial contact with a transducer [6]. In terms of food analysis, the binding partner interacts specifically with the contaminant of interest and produces some form of signal detected by the transducer. There are several forms of transducers available that can measure these interactions including those that detect electrochemical signals [7], mass/acoustic signals [8] and optical signals [9]. There are several different types of optical biosensors including those based on fluorescence [10], surface plasmon

resonance (SPR) [5] and biolayer interferometry [11]. In the present study, biolayer interferometry has been used to detect domoic acid, a low-molecular-weight contaminant found in shellfish but derived from algae.

Biolayer interferometry

Biolayer interferometry (BLI) employs a real-time, label-free, optical transducer that measures changes in interference patterns of light when reflected from the surface of an optical fibre [11]. The tip of an optical fibre is coated with a polymer facilitating covalent immobilisation of biospecific molecules as a biolayer. The optical fibre can then be placed into a liquid sample containing the antibody against the immobilised molecule, and white light is allowed to travel down the fibre into the sample solution. Some of the light, travelling down the fibre, will be reflected back by either the tip of the fibre or by the biolayer. These two reflected beams will interfere with each other leading to a shift in the wavelength detected by the photodetector. This shift is directly related to the distance between the two reflection surfaces, measured in terms of nanometres, and as such the thickness of the biolayer [11–15]. Only molecules binding to or dissociating from the tip can cause a shift in the interference pattern [13].

Concentration analysis for low-molecular-weight food contaminants

Domoic acid is a naturally occurring low-molecular-weight toxin, molar mass approximately 311 g/mol, produced by the diatoms of genera *Pseudonitzshia*, *Nitzschia* and *Chondria* [16]. The toxin can accumulate in shellfish and lead to amnesic shellfish poisoning in humans [16–18]. As a result, an action limit of 20 μg/g for domoic acid in edible bivalve molluscs was established by the European Union [19, 20].

It has previously been noted that, for concentration analysis of low-molecular-weight food contaminants, molecular weight<1,000 daltons by SPR requires the use of inhibition assays [21–23]. This is because the transducer is not sensitive enough to distinguish the binding of the small molecule to the surface at the levels of interest. Sandwich approaches are also ruled out since the molecules are so small that it is not possible for two antibodies to bind simultaneously to the target due to steric hindrance. Therefore, inhibition assays are utilised where a much larger signal can be produced when the small molecule is immobilised and inhibition is produced by interacting free small molecules in the sample with a limited concentration of its much larger antibody. On introduction of this mixture to the immobilised surface, any unbound antibody will be free to bind to the immobilised small molecule, thus producing a relatively larger signal than a direct approach. A similar approach can be applied when using biolayer interferometry to increase signal levels. In the present study, domoic acid is immobilised onto the surface, and the biosensor then dipped into solutions containing anti-domoic acid antibodies. When fixed concentrations of antibody are mixed with different concentrations of free domoic acid, calibration curves can be constructed because antibody binding to free domoic acid in solution will be inhibited from binding to the surface, thus the shift in interference pattern, which is related to the thickness of the biolayer, will be dependent on the calibrant concentration. The signal strength is inversely proportional to the concentration of domoic acid in solution.

The aim of this study is to provide proof-of-concept that BLI biosensors can be used to detect low-molecular-weight food contaminants, at a concentration of interest to analysts. Within this study, domoic acid was selected, as a model compound to investigate the instrument's performance characteristics and ascertain the effects, on the calibration curve, of manipulating assay parameters. Following optimisation, domoic acid calibration curves were produced in buffer and sample matrix to determine if the biosensor could detect domoic acid at a concentration of interest in matrix. Furthermore, observations were made on what influence sample extracts had on the system using the appropriate sample preparation.

Materials and methods

Reagents

Domoic acid was obtained from Fluorochem, UK. Amine coupling reagent kit, amine-reactive biosensors were obtained from ForteBio, UK. HEPES-buffered saline-EP (HBS-EP) buffer (assay buffer) was obtained from GE Healthcare, UK, 1-ethyl-3-[3-dimethylaminopropyl] carbodiimide hydrochloride (EDC), 2,2'-(ethylenedioxy)bis-(ethylamine) (jeffamine), *N*-hydroxysulfosuccinimide (NHS) and sodium hydroxide (regeneration solution) were obtained from Sigma-Aldrich UK.

Instrumentation

The Octet Red96 has been designed as a user-friendly benchtop-based instrument (footprint 47(H)×43(D)×53 cm(W)), developed by ForteBio Inc (Menlo Park, CA, USA), capable of reading signals from eight sensors simultaneously. It utilises BLI to achieve a dynamic range covering nanogram-per-millilitre to milligram-per-millilitre levels for quantification of biomolecules. It comes ready-to-use with dedicated easy-to-use acquisition and analysis software. The Octet Red96 utilises disposable Dip and Read™ biosensors in an 8×12-array format to perform measurements in 200 μl samples contained in 96-well microtitre plates [14, 24]. The instrument is fully automated, so the user simply positions the biosensor rack and microtitre plate in the appropriate positions and programs the method to be

performed. It can simulate liquid flow via orbital shaking of the sample microtitre plate [25].

Determination of instrument performance characteristics

Production of anti-domoic acid antibodies

Polyclonal antibodies were prepared using a domoic acid–bovine thyroglobulin protein conjugate in the same manner as that described by Traynor et al. [19]. The antibody was purified by ammonium sulphate precipitation followed by dialysis, and the protein concentration was determined to be 4.9 mg/ml.

Immobilisation of domoic acid onto biosensors

Dip and Read™ amine-reactive biosensors were used for all experiments. These biosensors can be regenerated and have a carboxylate group polymer layer that facilitates immobilisation via standard amine coupling chemistry. All immobilisations were performed offline under gentle agitation and in humid conditions. Reagents were contained in the wells of a microtitre plate, and 200 μl volumes for each biosensor were used throughout. Biosensors tips were pre-soaked in 0.1 M MES buffer, pH 5.0, for 30 min. EDC and NHS solutions were prepared according to the instructions in the amine coupling reagent kit and mixed 1:1 before being used to activate the surface for 30 min. Biosensors were then placed into 0.1 M jeffamine for 2 h followed by 1 M ethanolamine pH 8.5 for a further 30 min. Meanwhile, reaction mixtures were prepared that would scale to produce 200 μl solutions of the following recipe for each biosensor to be immobilised. Domoic acid (0.1 mg) was activated by the addition of EDC (0.17 mg) and NHS (0.07 mg) in 0.1 M MES buffer, pH 5.0 (200 μl). The mixture was allowed to react for 30 min at room temperature, protected from light, before the pH was adjusted to 7. Each individual biosensor was then placed in a 200-μl aliquot and allowed to react overnight. The following day biosensors were allowed to equilibrate in HBS-EP buffer before analysis.

Binding and inhibition experiments

Initial experiments were performed, on three domoic acid-immobilised biosensors, to see if both binding and inhibition could be observed. Antibody was diluted 1/100 and mixed 1:1 with either assay buffer (HBS-EP) or 100 ng/ml domoic acid standard. A method was set up whereby oscillation was set at 1,000 revolutions per minute (rpm) and baseline signal measured, in assay buffer, for 5 min, followed by the biosensors being placed in the negative sample for 20 min association, followed by 100-s dissociation in assay buffer. The biosensors were then regenerated using 100 mM sodium hydroxide for 5 s before the cycle was repeated, this time dipping the sensors into the domoic acid-positive sample.

Optimisation of biosensor parameters

Following the initial assessment of performance characteristics, the assay development potential of the instrument was investigated by altering assay parameters (antibody concentration, association time, derivative concentration and oscillation speed) to ascertain their effects on the assay midpoint and dynamic ranges as judged by calibration curves generated. Other parameters (calibrants, assay temperature, baseline, dissociation and regeneration time) remained unchanged for the repeatability experiments described later. Each of the altered parameters was modified in turn to determine what effect it would have on the calibration curve. Finally, a combination of the most influential parameters was assessed.

Repeatability

Repeatability was tested using six individual biosensors, immobilised with domoic acid, to simultaneously produce six calibration curves. Anti-domoic acid polyclonal antibody was diluted 1/100 and mixed with domoic acid standards ranging between 100 and 0 ng/ml (n=5). Aliquots were then placed in rows on a microtitre plate before analyses were performed in duplicate (total 10 cycles per biosensor). A method was developed whereby the microtitre plate was set to shake at 1,000 rpm at 25 °C. The biosensor baseline reading was performed in assay buffer for 5 min before the six biosensors were transferred, to the first row of samples, and association allowed to progress for 10 min before the biosensors were returned to buffer for 100 s to allow dissociation. The biosensors were then regenerated for two 5-s periods in 100 mM sodium hydroxide, then assay buffer in preparation for the next cycle. The data were prepared for analyses by subtracting the average signals from two reference biosensors (immobilised similar to other sensors only without domoic acid), from each cycle, then all cycles were baseline-aligned and a report point taken 30 s into the dissociation phase. Report point information was then imported into BIAEvaluation software for the production of calibration curves using a four-parameter fit.

Reproducibility

Reproducibility was tested by running three calibration curves on three separate days using the same assay procedure as described under the "Repeatability" section, excluding subtraction of reference biosensors, since this procedure did not affect the final result. Freshly prepared reagents and sensors were used on each occasion.

Comparison of buffer and matrix calibration curves

The optimised assay conditions (antibody 1/400, 10 min association time, 1,000 rpm microtitre plate oscillation at

25 °C, biosensors immobilised with 0.5 mg/ml derivative, 100 s dissociation time and two 5-s period regenerations with 100 mM sodium hydroxide and assay buffer) were used to simultaneously produce calibration curves in buffer and mussel tissue extracts. One set of samples was spiked before extraction and one spiked after extraction. Antibody was mixed 1:1 with calibrants ranging from 20 to 0 ng/ml (20, 10, 2, 1, 0.5 and 0 ng/ml). Calibrants were processed in duplicate and report points taken during baseline and 30 s into dissociation. Report point information was imported into BIAEvaluation software V4.1 (GE Healthcare UK) for construction of calibration curves using a four-parameter fit.

Preparation of mussel samples (spiked before extraction)

The EU action limit for domoic acid is 20 μg/g of mussel tissue. Sample preparation was used that facilitated a 1-g sample spiked at this action limit to be positioned close to the midpoint (2.0 ng/ml) of the buffer calibration curve using the assay conditions above. Calibrants were prepared by weighing 1 g mussel into a centrifuge tube, then spiked with the appropriate concentration of domoic acid stock solution to prepare samples containing 200, 100, 20, 10, 5 and 0 μg/g. After 30 min, 4 ml of water was added and the sample homogenised, then gently mixed for 30 min on a roller mixer followed by centrifugation at 3,000×*g* for 5 min. Sample aliquots then underwent a two-step serial dilution (facilitating a further 1/2,000 dilution), meaning that the spiked samples were now 20, 10, 2, 1, 0.5 and 0 ng/ml calibrants, respectively.

Preparation of mussel samples (spiked after extraction)

A negative mussel sample was taken through the full sample preparation described above, including 1/2000 dilution, then 950 μl aliquots were spiked with 50 μl of appropriate spiking solution to prepare 20, 10, 2, 1, 0.5 and 0 ng/ml calibrants.

Results and discussion

Determination of instrument performance characteristics

A raw data sensorgram showing five complete cycles for six simultaneous biosensors is provided in Fig. 1. The inhibition assay principle can be seen with the increase in signal (nanometres) with decreasing concentrations in the domoic acid standards.

Binding and inhibition experiments

An average signal (n=3) of 1.8603 nm (4.1 %CV) was observed for the negative sample whilst 0.4371 nm (5.3 %CV) was obtained for the positive thus providing a difference of 1.4232 nm (i.e. a 77 % signal inhibition) between zero and 100 ng/ml domoic acid. This proved that

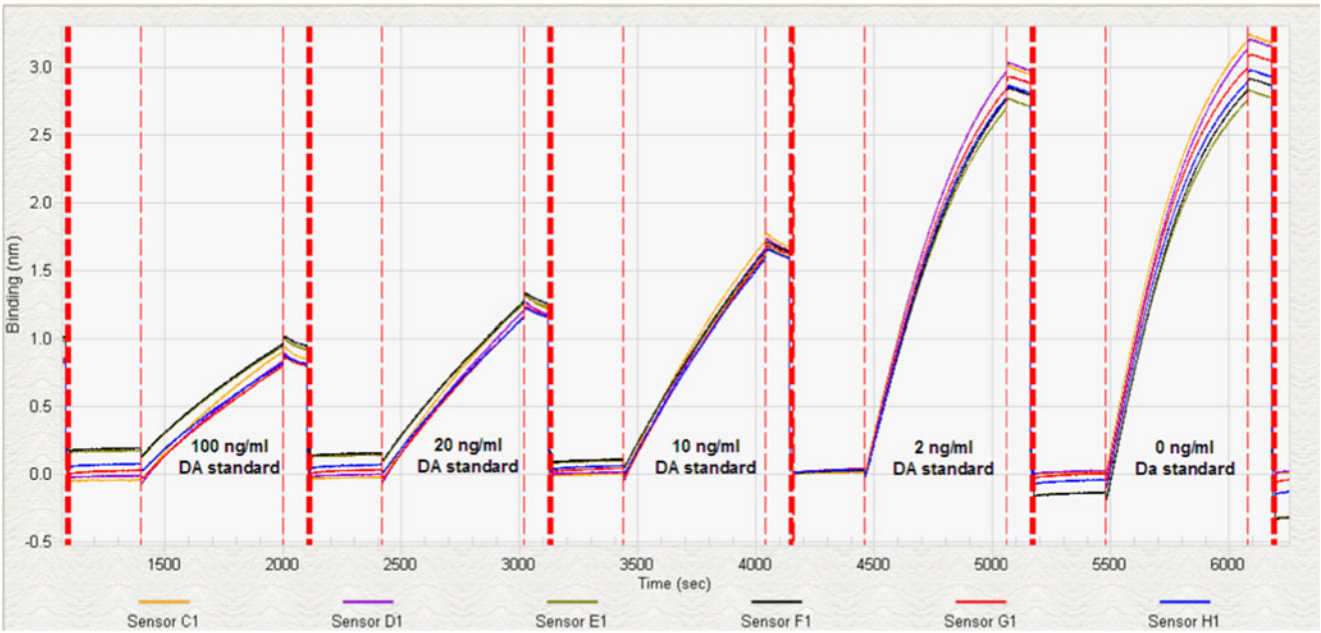

Fig. 1 Raw data sensorgram showing binding profiles for five different domoic acid concentrations. Data for sensors C1 to H1 produced simultaneously. Antibody diluted 1/100 and mixed with each standard. Each cycle shows 5 min baseline, 10 min association and 100 s dissociation followed by regeneration in preparation for the next cycle. A typical inhibition profile is observed with high standard concentrations yielding low signals while lower standard concentrations yield relatively high signals

the binding of the antibody to the surface was detected as well as its inhibition due to the presence of domoic acid in solution. It was decided that a 20 min association time was too long, and so this was reduced to 10 min for the production of calibration curves and testing of repeatability and reproducibility.

Optimisation of biosensor parameters

Table 1 outlines the findings of the experiments whereby parameters were varied to ascertain the effect on the calibration curve. Replicates (n=2) for each calibrant, in individual calibration curves, ranged from 0.0 to 9.9 %CV. Signal range (nanometres) and midpoints (nanograms per millilitre) of each calibration curve were compared to see the affect of altering that parameter (for example, antibody dilution or association time) on the calibration curve. In terms of assay performance, both signal range and midpoint values are useful parameters to evaluate. A large range provides for improved resolution of concentration within the calibration curve. With a larger signal range, over the linear section, small changes in signal will not lead to large variations in calculated concentration whereas a lower signal range between the same calibrants will mean that a small shift in signal will lead to larger changes in calculated concentrations and potentially increased %CVs of replicates. Midpoint analysis is a useful tool in assessing the calibration curves overall performance. It involves comparing different calibration curves at a fixed point in their linear range (the midpoint). A decrease in midpoint value indicates that a curve has shifted towards being more sensitive for lower concentrations of analyte and potentially a lower detection limit. The signal range between the strongest and weakest calibrants, the midpoint and calibrant replicates (%CV) for antibody dilution 1/100, derivative concentration 0.5 mg/ml, microtitre plate agitation 1,000 rpm at 25 °C and association time 10 min were use as reference values to assess the effects of the assay alterations.

Increasing antibody dilution (Table 1, rows 1–3)

As expected, increasing antibody dilution caused a drop in signal range between the strongest and weakest calibrants. This is because increasing antibody dilution means there is less total antibody present that could interact with the surface, and also, it will require lower concentrations of calibrant to inhibit antibody interactions with the surface. The range dropped from 1.8326 nm between strongest and weakest calibrants for a 1/100 dilution to 0.8115 nm for a 1/400 dilution. This value obtained was 44 % of that obtained for the 1/100 antibody. Increasing antibody dilution also lowered the calibration curve midpoint, shifting it left towards lower concentrations and potentially lowering the limit of detection, as can be seen by the midpoint dropping from 7.2 to 2.0 ng/ml. This is because it takes decreasing concentrations of calibrant to inhibit binding to the surface as antibody dilution is increased thus improving sensitivity at lower concentrations. Interestingly, the CVs

Table 1 Effects of varying assay parameters on domoic acid calibration curves range, midpoint and %CV for calibrant replicates (n=2)

Row	Antibody dilution	Association time (min)	rpm	Derivative concentration (mg/ml)	Range (nm)	Curve Midpoint (ng/ml)	Calibrant replicates (n=2)%CV
1	1/100	10	1,000	0.5	1.8326	7.2	3.3 to 5.9
2	1/200	10	1,000	0.5	1.4899	3.7	1.6 to 3.5
3	1/400	10	1,000	0.5	0.8115	2.0	0.4 to 1.1
4	1/100	10	1,000	0.5	1.8326	7.2	3.3 to 5.9
5	1/100	10	1,000	0.1	1.1835	8.0	2.8 to 6.0
6	1/100	10	1,000	0.02	0.3213	9.9	1.2 to 9.1
7	1/100	10	1,000	0.5	1.8326	7.2	3.3 to 5.9
8	1/100	10	500	0.5	1.6019	6.1	1.8 to 5.0
9	1/100	10	250	0.5	0.9943	5.6	0.3 to 1.4
10	1/100	5	1,000	0.5	1.3835	5.7	0.0 to 1.2
11	1/100	10	1,000	0.5	1.8502	7.5	3.8 to 5.2
12	1/100	20	1,000	0.5	1.8823	10.4	7.3 to 9.9
13	1/200	5	250	0.5	0.2732	4.0	1.1 to 3.3
14	1/400	5	250	0.5	0.1429	2.5	0.6 to 4.8
15	1/600	5	250	0.5	0.0937	1.9	0.7 to 7.8

Varying antibody concentration: rows 1–3; varying immobilised derivative concentration: rows 4–6; altering oscillation speed: rows 7–9; adjusting association time: rows 10–12; combining most influential adjustments: rows 13–15. Results from rows 1, 4, 7 and 11 are set as reference for each individual variation

for replicates (n=2) also improved with increased antibody dilution.

Decreasing derivative concentration (Table 1, rows 4–6)

As expected, the signal range between strongest and weakest calibrants decreased with decreasing concentrations of domoic acid immobilised on the surface. This is because the activity of the surface becomes the limiting factor. For concentration analysis, it is advisable that the sensor surface should be densely immobilised so that reduced surface molecules are not the limiting factor in the assay. The range dropped from 1.8326 nm between strongest and weakest calibrants when 0.5 mg derivative was used to 0.3213 nm when 0.02 mg derivative was used for immobilisation. This value is 17.5 % of the range obtained with 0.5 mg derivative. The curve was also slightly shifted right, towards higher concentrations, shown by a shift in midpoint from 7.2 to 9.9 ng/ml. Meanwhile the spread in %CV associated with the calibrant replicates (n=2) increased contra to what was observed with %CVs observed with decreasing range caused by increased antibody dilution. The 9.1 %CV was for the replicates for the strongest calibrant which gives the lowest signal in the calibration curve (data not shown) so higher %CVs were expected.

Decreasing rpm of microtitre plate oscillation (Table 1, rows 7–9)

Decreasing oscillation caused the calibrant signal range to be reduced to 54 % of the initial level. However, the curves shifted slightly left, towards lower concentrations, with the midpoint moving from 7.2 to 5.6 ng/ml. The signal range for calibrants changed in a similar intensity as that produced for changing antibody dilution, but the corresponding alteration to the midpoint was not reflected. Therefore, altering the antibody dilution has more influence than altering rpm. Again, the calibrant replicates %CV showed improvements with decreasing rpm.

Altering association time (Table 1, rows 10–12)

Halving the association time to 5 min caused the signal range to decrease to 75 % of the starting range but slightly lowered the curve midpoint to 5.7 ng/ml. Doubling the association time to 20 min increased the range to 102 % of the initial value but shifted the curve right, towards higher concentrations, as seen in a shift in midpoint to 10.4 ng/ml. The 5 min association time also provided the best %CV values for calibrant replicates. From these data, it can be observed that shorter association times can shift the calibration curve left towards lower concentrations whilst increasing the time does not necessarily increase the range significantly and will shift the curve right, towards higher concentrations.

Combining variables to achieve lowest midpoint (Table 1, rows 13–15)

A combination of the parameters that lowered the midpoint were applied. When altering parameters individually, the lowest midpoints were obtained using 0.5 mg/ml derivative, 250 rpm, 5 min association times and increased antibody dilution factor. Decreasing rpm and association time and increasing dilution factor all reduce the signal (data not shown) and signal range between strongest and weakest calibrants, thus increasing the probability that the calibration curve fit would fail; therefore, several antibody dilutions were investigated. As expected, the signal range decreased as the dilution factor was increased, and likewise, the midpoint was lowered indicating increased sensitivity at lower concentrations and potentially a lower detection limit. The spread of the %CV increased with dilution factor. This is to be expected with decreasing signal levels. Small variations in replicates were manifested as higher %CVs.

Of all the parameters studied, the antibody dilution factor had the biggest influence on midpoint and signal ranges. The minimal effects of other parameters on the midpoint, such as association time and oscillation speed, can be seen by comparing rows 2 and 13 of Table 1. Adjusted individually, these parameters decreased midpoint, but when combined, there is very little difference (row 2, 3.7 ng/ml; row 13, 4.0 ng/ml), and if anything, it slightly shifts the sensitivity towards higher concentrations. The signal range has also been substantially reduced to 18 % of that shown for the conditions in row 2. Preferentially, a larger range would be desirable allowing for better concentration resolution. A similar picture was observed between rows 3 and 14.

The lowest midpoint obtained (1.9 ng/ml) was for the conditions outlined in Table 1 row 15. This is only 0.1 ng/ml lower than that obtained for the conditions in row 3 (2.0 ng/ml). The signal range is superior in row 3 (row 15 signal range is 11.5 % of that observed in row 3) and %CV generally better. This would all suggest that producing a calibration curve with the conditions in row 3 would lead to a more robust curve than one produced using row 15 conditions with practically no change in curve midpoint and detection limit.

Repeatability

Figure 2 shows an overlay of the six calibration curves, in duplicate, produced from the repeatability data and shows very good levels of repeatability. Table 2 shows statistical analysis for the repeatability experiment. CVs for calibrant replicates (n=2), for each biosensor, ranged from 0.1 to

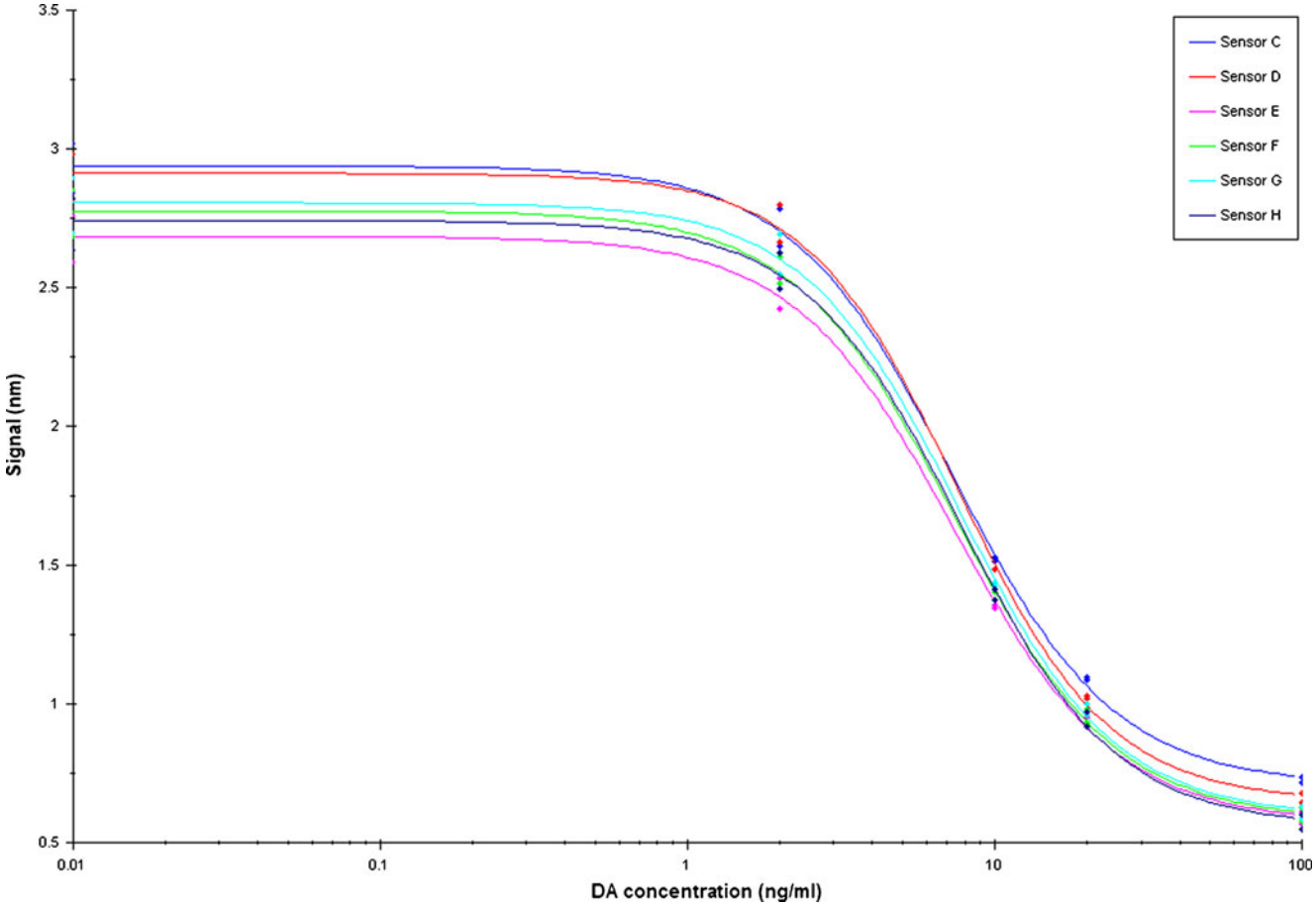

Fig. 2 Domoic acid calibration curve overlay showing repeatability for six sensors (C1 to H1). Signal at report point is plotted against concentration of standard. Each calibration curve was constructed from report points taken during each cycles dissociation phase relative to baseline. Report point signals were imported into BIAEvaluation software and calibration curves constructed using a four-parameter-fit equation

6.5 %. The CV for each concentration across all six biosensors (n=12) ranges from 4.3 to 9.3 % showing that the calibration curves generated were very reproducible. Considering these CVs in a screening assay protocol, it may be possible to produce a calibration curve using data from different sensors, thus providing more microtitre plate

Table 2 Repeatability data for six sensors ran simultaneously producing six domoic acid calibration curves

		Sensor location and signal (nm)							
Concentration (ng/ml)	Replicate	C	D	E	F	G	H	Mean signal (n=12)	%CV (n=12)
100	1	0.7176	0.6437	0.5694	0.5760	0.5893	0.5504	0.6277	9.3
	2	0.7375	0.6782	0.6106	0.6256	0.6313	0.6031		
20	1	1.0844	1.0194	0.9246	0.9350	0.9646	0.9178	0.9898	5.9
	2	1.0951	1.0305	0.9545	0.9820	0.9980	0.9715		
10	1	1.5276	1.4847	1.3481	1.3765	1.4261	1.3752	1.4299	4.3
	2	1.5158	1.4859	1.3589	1.4071	1.4382	1.4144		
2	1	2.7818	2.8000	2.5329	2.6104	2.6937	2.6242	2.6106	4.4
	2	2.6486	2.6608	2.4219	2.5133	2.5461	2.4940		
0	1	3.0185	2.9784	2.7580	2.8505	2.8915	2.8222	2.7986	4.7
	2	2.8399	2.8177	2.5915	2.6839	2.6951	2.6357		
Range (nm)		2.2016	2.2371	2.0848	2.1664	2.1830	2.1521		
Midpoint (ng/ml)		7.3	7.6	7.4	7.3	7.7	7.7		

positions for actual samples. In the format used for the repeatability experiment, eight rows in total are needed for the production of six calibration curves (one for baseline, five for calibrants and one each for regeneration and wash) leaving only four wells in each column for samples. If a calibration curve and samples could be run using different biosensors and combined for analysis, then the number of sample positions could increase dramatically. Midpoint values were also determined for each calibration curve showing an average of 7.5 ng/ml with a CV of 2.3 % (n=6). Although not directly comparable, these repeatability data show similar variation to that produced by Maragos [11], who used BLI to detect deoxynivalenol in whole wheat flour and other optical biosensor methods such as those produced by Meneely et al. [22], using a SPR biosensor for the detection of T-2 and HT-2 toxin in cereals and maize-based baby food.

Reproducibility

Table 3 shows the reproducibility data for three calibration curves processed on three separate days. CVs for individual replicates (n=2) range from 2.0 to 6.5 %. The calibration curve on day 1 shows slightly elevated signals (nanometre) for the calibrants and a larger range compared with days 2 and 3. This would indicate that a calibration curve produced on day 1 could not be used to read samples prepared on different days. However, the CV of the midpoint concentration (n=3) is only 3.4 %, indicating that, although the signal and range may be different, it has little effect on the reproducibility of the calibration curve.

Comparison of buffer and matrix calibration curves

Figure 3 shows an overlay plot of the simultaneously produced calibration curves in buffer and matrix. As can be seen, the buffer curve and the extracted samples practically overlay each other over the majority of the calibration curve with the spiked after extraction curve sitting slightly higher. Replication (n=2) of calibrants was very good, 0.1 to 2.7 %CV for buffer curve, 0.1 to 2.8 %CV for extracted curve and 0.6 to 2.1 %CV for calibrants spiked after extraction. Midpoint values for buffer curve, extracted curve and spiked after extraction curve were 1.7, 1.8 and 2.0 ng/ml, respectively, with signal ranges of 0.8113, 0.7604 and 0.7470 nm between strongest and weakest calibrant. For the two matrix curves, the midpoint values were equivalent to 18 and 20 μg/g domoic acid is tissue, respectively, when sample preparation was taken into consideration. The calibration curve midpoint values are similar to those reported by Campbell et al. [26] (domoic acid midpoint 2.6 ng/ml), who used a multiplexing array SPR biosensor to detect both large- and small-molecular-weight compounds, and superior to those produced by Le Berre and Kane, Micheli et al., Stevens et al. and Yu et al. [17, 21, 27, 28] (midpoint approximately 20 ng/ml using SPR biosensors or electrochemical biosensor in the case of Micheli et al. [27]), Kreuzer et al. [29] (midpoint approximately 40 ng/ml using an electrochemical biosensor) and Lotierzo et al. [30] (midpoint approximately 60 ng/ml using a SPR biosensor). However, as can be seen when comparing these to Traynor et al. [19] (midpoint approximately 18 μg/g using a SPR biosensor), who used the equally valid approach of producing an assay with optimal sensitivity close to the action limit, all the previously mentioned assays are capable of detecting domoic acid at its action limit through the use of appropriate sample dilution steps.

The data would suggest that, using this sample preparation and assay conditions, it should be possible to use a buffer curve to screen real samples with the action limit close to the midpoint of the calibration curve, giving optimum concentration resolution around this value. This is contra to the findings of Maragos [11] who suggest that matrix-matched calibration curves are required for their

Table 3 Domoic acid reproducibility

	Day 1		Day 2		Day 3	
Concentration (ng/ml)	Signal (nm)	%CV	Signal (nm)	%CV	Signal (nm)	%CV
100	0.5504 0.6031	6.5	0.4450 0.4096	5.9	0.4713 0.4380	5.2
20	0.9178 0.9715	4.0	0.7463 0.7121	3.3	0.7915 0.7505	3.8
10	1.3752 1.4144	2.0	1.1147 1.0627	3.4	1.1758 1.1127	3.9
2	2.6242 2.4940	3.6	2.1371 2.0106	4.3	2.2067 2.0602	4.9
0	2.8222 2.6357	4.8	2.3350 2.1849	4.7	2.3793 2.2304	4.6
Range (nm)	2.1521		1.8326		1.8502	
Midpoint (ng/ml)	7.7		7.2		7.5	

Produced by repeating a calibration curve on different days using freshly prepared reagents and biosensors

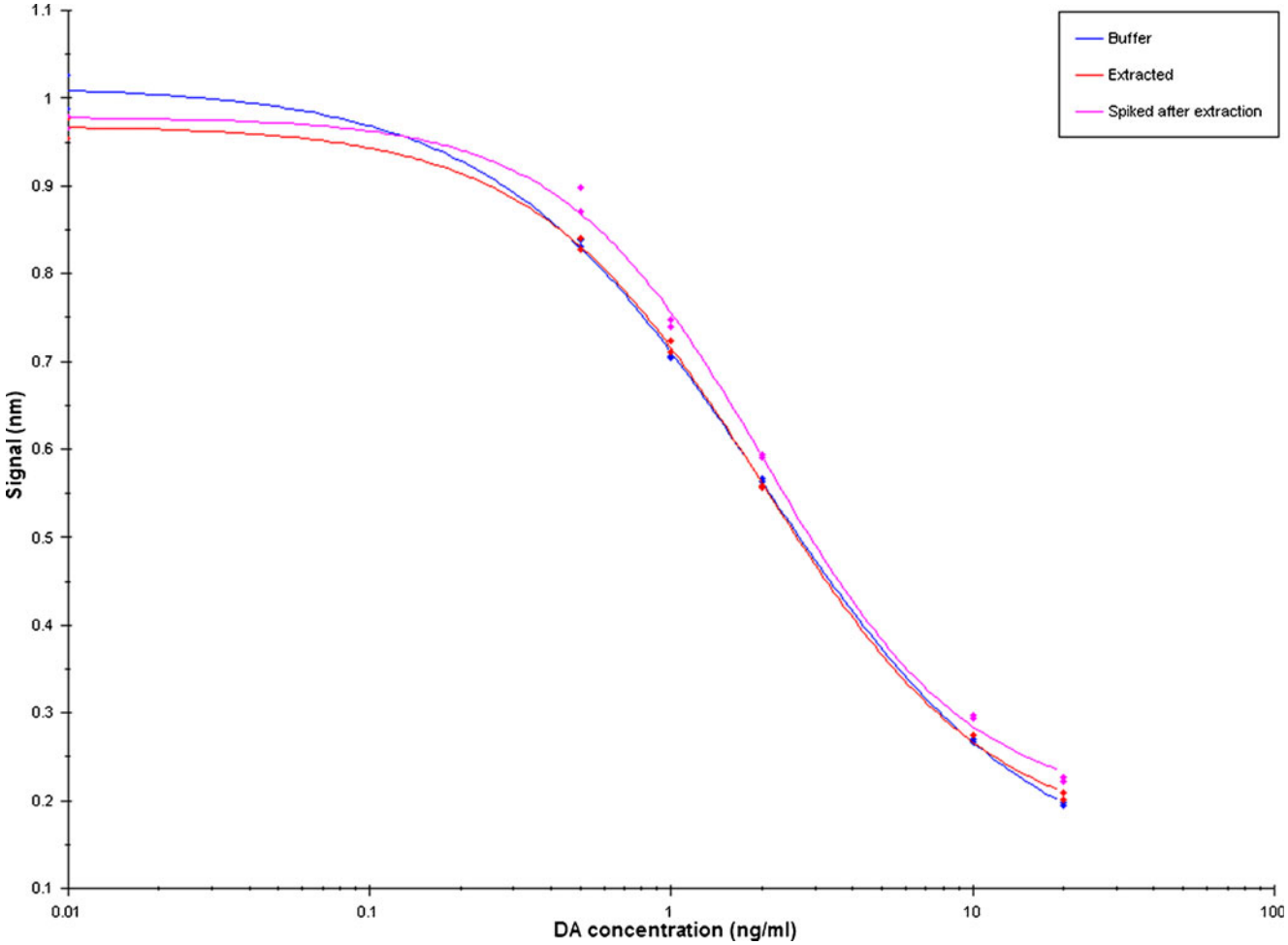

Fig. 3 Calibration curve overlay showing calibration curves in buffer, extracted from mussel and spiked after sample preparation. Signal at report point is plotted against concentration of standard. Each calibration curve was constructed from report points taken during each cycles dissociation phase relative to baseline. Report point signals were imported into BIAEvaluation software and calibration curves constructed using a four-parameter fit equation

work on the detection of deoxynivalenol in whole wheat flour. This difference in findings can be accounted for by the different techniques used for sample preparation, specifically the dilution step. The sample preparation of Maragos [11] left a more concentrated sample. Following initial preparation, the wheat sample was diluted 1/5 compared with a 1/2,000 dilution applied after the initial mussel preparation in this study. The use of a calibration curve with high sensitivity at low concentrations and the application of a large dilution mean that potential matrix interference was practically eliminated in the mussel samples. With this simple and solvent-free sample preparation, it is feasible to locate the biosensor on a ship and use it to screen for contaminated mussels at the harvesting site before samples are returned to shore, thus saving time and costs associated with detecting inappropriate contamination levels at land-based laboratories.

Conclusion

Data have been presented providing proof-of-concept for the use of BLI as a useful screening tool for the detection of domoic acid with repeatability and reproducibility values similar to previously published instrument performance data. By using domoic acid as a low-molecular-weight model compound, it could be further concluded that BLI shows the potential to be used as a screening tool for other low-molecular-weight food contaminants. Assay development procedures have shown the influence of various adjustable assay parameters on assay performance. The detection capability achieved using BLI is similar to, or better than, those achieved in previously published optical and electrochemical biosensor assays for the detection of domoic acid. It has also been shown that it should be possible to analyse mussel samples for domoic acid contamination without the need for matrix-matched calibration curves.

Acknowledgements The authors would like to thank Sriram Kumaraswamy, Philip Buckle and Krista Witte (Fortebio, A Division of Pall Life Sciences) for their help and guidance on working with the Octet Red96 system.

Funding for the project was provided by the Department of Employment and Learning for Northern Ireland as part of the ASSET Centre project.

References

1. Huang C, Dostalek J, Sessitsch A et al (2011) Long-range surface plasmon-enhanced fluorescence spectroscopy biosensor for ultra-sensitive detection of *E. coli* O157:H7. Anal Chem 83:674–677
2. Ferguson J, Baxter A, Young P et al (2005) Detection of chloramphenicol and chloramphenicol glucuronide residues in poultry muscle, honey, prawn and milk using a surface Plasmon resonance biosensor and qflex((R)) kit chloramphenicol. Anal Chim Acta 529:109–113
3. Fodey T, Murilla G, Cannavan A et al (2007) Characterisation of antibodies to chloramphenicol, produced in different species by enzyme-linked immunosorbent assay and biosensor technologies. Anal Chim Acta 592:51–57
4. Chen B, Ma M, Su X (2010) An amperometric penicillin biosensor with enhanced sensitivity based on co-immobilization of carbon nanotubes, hematein, and beta-lactamase on glassy carbon electrode. Anal Chim Acta 674:89–95
5. Fernandez F, Pinacho DG, Sanchez-Baeza F et al (2011) Portable surface plasmon resonance immunosensor for the detection of fluoroquinolone antibiotic residues in milk. J Agr Food Chem 59:5036–5043
6. McGrath TF, Elliott CT, Fodey TL (2012) Biosensors for the analysis of microbiological and chemical contaminants in food. Anal Bioanal Chem 403:75–92
7. Paniel N, Radoi A, Marty JL (2010) Development of an electrochemical biosensor for the detection of aflatoxin M1 in milk. Sensors 10:9439–9448
8. Salmain M, Ghasemi M, Boujday S et al (2011) Piezoelectric immunosensor for direct and rapid detection of staphylococcal enterotoxin A (SEA) at the ng level. Biosens Bioelectron 29:140–144
9. Indyk HE (2011) An optical biosensor assay for the determination of folate in milk and nutritional dairy products. Int Dairy J 21:783–789
10. Taitt CR, Shriver-Lake LC, Ngundi MM et al (2008) Array biosensor for toxin detection: continued advances. Sensors 8:8361–8377
11. Maragos C (2011) Detection of deoxynivalenol using biolayer interferometry. Mycotoxin Rese 27:157–165
12. Concepcion J, Witte K, Wartchow C et al (2009) Label-free detection of biomolecular interactions using BioLayer interferometry for kinetic characterization. Comb Chem High T Scr 12:791–800
13. Cattepoel S, Hanenberg M, Kulic L et al (2011) Chronic intranasal treatment with an anti-a beta(30–42) scFv antibody ameliorates amyloid pathology in a transgenic mouse model of Alzheimer's disease. PLoS One 6:e18296
14. Wilson JL, Scott IM, McMurry JL (2010) Optical biosensing. Biochem Mol Biol Edu 38:400–407
15. Nirschl M, Reuter F, Vörös J (2011) Review of transducer principles for label-free biomolecular interaction analysis. Biosensors 1:70–92
16. Vilarino N, Fonfria ES, Carmen Louzao M et al (2009) Use of biosensors as alternatives to current regulatory methods for marine biotoxins. Sensors 9:9414–9443
17. Le Berre M, Kane M (2006) Biosensor-based assay for domoic acid: comparison of performance using polyclonal, monoclonal, and recombinant antibodies. Anal Lett 39:1587–1598
18. Syaifudin ARM, Mukhopadhyay SC, Jayasundera KP (2008) Electromagnetic interaction of planar interdigital sensors with chemicals contaminated in seafood. Sensing Technology, 2008. ICST 2008. 3rd International Conference on :620–625
19. Traynor I, Plumpton L, Fodey T et al (2006) Immunobiosensor detection of domoic acid as a screening test in bivalve molluscs: comparison with liquid chromatography-based analysis. J AOAC Int 89:868–872
20. Regulation (EC) No 853/2004 of the European Parliament and of the Council of 29 April 2004 laying down specific hygiene rules for food of animal origin (OJ L 139, 30.4.2004, p. 55), consolidated version 2011-12-29.
21. Yu Q, Chen S, Taylor A et al (2005) Detection of low-molecular-weight domoic acid using surface plasmon resonance sensor. Sensor Actuat B-Chem 107:193–201
22. Meneely JP, Sulyok M, Baumgartner S et al (2010) A rapid optical immunoassay for the screening of T-2 and HT-2 toxin in cereals and maize-based baby food. Talanta 81:630–636
23. Haughey SA, Elliott CT, Oplatowska M et al (2012) Production of a monoclonal antibody and its application in an optical biosensor based assay for the quantitative measurement of pantothenic acid (vitamin B5) in foodstuffs. Food Chem 143:540–545
24. ForteBio (2012) Octet® RED96 system. Available via http://www.fortebio.com/octet_RED96.html. Accessed March 6 2012
25. ForteBio (2012) Octet® RED96 system specifications. Available via http://www.fortebio.com/octet_red96_specs.html. Accessed March 6 2012
26. Campbell K, McGrath T, Sjölander S et al (2011) Use of a novel micro-fluidic device to create arrays for multiplex analysis of large and small molecular weight compounds by surface plasmon resonance. Biosens Bioelectron 26:3029–3036
27. Micheli L, Radoi A, Guarrina R et al (2004) Disposable immunosensor for the determination of domoic acid in shellfish RID C-5820-2011 RID A-4504-2008. Biosens Bioelectron 20:190–196
28. Stevens RC, Soelberg SD, Eberhart BL et al (2007) Detection of the toxin domoic acid from clam extracts using a portable surface plasmon resonance biosensor. Harmful Algae 6:166–174
29. Kreuzer M, Pravda M, O'Sullivan C et al (2002) Novel electrochemical immunosensors for seafood toxin analysis. Toxicon 40:1267–1274
30. Lotierzo M, Henry O, Piletsky S et al (2004) Surface plasmon resonance sensor for domoic acid based on grafted imprinted polymer RID E-2573-2011. Biosens Bioelectron 20:145–152